STATISTICS, OPTIMIZATION AND INFORMATION COMPUTING
Stat., Optim. Inf. Comput., Vol. **16**, July 2026, pp 660–683.
Published online in International Academic Press (www.IAPress.org)

Novel Quantile Regression Model Using Extended Exponential-Geometric Distribution with Real Data Application

Amal Sadeq Hamoodi [1], Ahmed Mahdi Salih [2,*]

[1]*Mathematics Department, College of Education ,Mustansiriya University, Iraq*
[2]*Department of Statistics, College of Administration and Economics, Wasit University, Kut, Iraq*

Abstract The current work proposes a quantile regression framework that takes into consideration the nature of the dependent variables that are characterized by restriction of the interval between 0 and 1, precisely by using the Unit Extended Exponential Geometric (UEEG) distribution. The method has the capacity to capture the effects of covariates at various quantiles of the distribution, allowing a more comprehensive representation of the changes in behavior across the whole range. We analyze the distribution characteristics of the model and recommend maximum likelihood parameter estimation. A simulation experiment is performed to test the properties of the proposed estimators at finite samples with respect to bias and MSE. The methodology is demonstrated through the application to a real data set in order to showcase its practical utility. The new framework is compared against the analogous ones based on Unit Exponential, Unit Extended Exponential, and Unit Lindley distributions using the Akaike information criterion (AIC), Bayesian information criterion (BIC), and Hannan Quinn information criterion (HQIC). The findings suggest that not only does the new model fit the data better, but it is also less biased and has a lower MSE, therefore, providing more flexibility for data restricted to a unit interval.

Keywords Quantile Regression, Unit Extended Exponential-Geometric, Residual Analysis, Pearson Residual

AMS 2010 subject classifications 62Jxx

DOI: 10.19139/soic-2310-5070-3802

1. Introduction

Quantile regression is a significant statistical tool that has been growing in usage to explore the relationship between explanatory variables and various parts of the conditional distribution of a response variable, rather than being limited to the conditional mean only. This characteristic of quantile regression renders it exceptionally suitable for scenarios where the data show heterogeneity, skewness, heavy tails, or bounded support, i.e., situations where classical mean-based regression models can offer incorrect or incomplete inference. Over the past few years, there have been extensive methodological innovations in quantile regression, for example, fully parametric models have been created which are based on probability distributions that are naturally related to the data structures such as proportions, survival times, and bounded responses on the unit interval (0,1).

Several parametric quantile regression models for bounded and unit-interval data were suggested by reparameterization the existing distributions in terms of quantiles and connecting these quantiles to covariates through appropriate link functions. A significant contribution in this direction was that of Jodrá and Jiménez-Gamero[18]. (2020) who devised a quantile regression model based on the Exponential-Geometric distribution for bounded responses and thus, paved the way for distribution-based regression frameworks that focus directly on conditional quantiles rather than moments.

*Correspondence to: Ahmed Mahdi Salih (Email: amahdi@uowasit.edu.iq). Department of Statistics, College of Administration and Economics, Wasit University, Kut, Iraq (5001)

ISSN 2310-5070 (online) ISSN 2311-004X (print)

In line with this framework, an increasing number of articles have extended parametric quantile regression to various distribution families and modeling frameworks.

Mazucheli et al[25]. (2022) offered a detailed review of parametric quantile regression models for unit-interval and positive data pointing out the implementation features and real-data applications. Santoro et al[30]. (2024) introduced the unit-power half-normal distribution in a quantile regression framework for healthcare data, and Bashir et al[9]. (2024) proposed a bounded exponentiated Weibull distribution and its quantile regression model demonstrating that it provides more flexibility for unit-supported responses. Besides these, there is also the unit-Chen quantile regression model Korkmaz et al [22]. (2023), the unit-Cauchy quantile regression model for proportion data Arslan and Yu [8]. (2025), and the exponentiated Weibull quantile regression model with cure-rate effects in survival analysis Gómez and Gallardo [15] (2025). Furthermore, the contributions of Wu and Rui [33] (2025) have also dealt with environmental and lifetime data by way of contamination unit models with quantile regression and quantile residual life regression under length-biased censoring.

Earlier and parallel research has also significantly contributed to the development of this area. Korkmaz [21] 2021 presented an exponential-power quantile regression model suitable for bounded data along with residual diagnostics. On the other hand, Sánchez et al [31]. (2021) suggested the use of a Weibull-based quantile regression framework accompanied by a comprehensive diagnostic analysis. Apart from unit-interval models, other approaches to distribution-based regression have been considered. These include finite mixture quantile regression for semi-continuous longitudinal data Maruotti et al [23]. (2020), log-symmetric quantile regression models for positive data Saulo et al [32]. (2020), and parametric quantile regression models for double-bounded responses Gallardo et al [14]. (2021). More general parametric methods based on versatile families such as the generalized gamma distribution have further pointed out how quantile regression can be used to model asymmetric and heterogeneous data features.

New achievements have also made it possible for quantile regression to reach unit distributions supported on boundaries, for example, the unit log-log model, as well as through the prevalent use of baseline distributions like the unit-Weibull in parametric quantile regression frameworks. Besides, the family of comprehensive distributional regression methods including GAMLSS focus on the whole conditional distribution by connecting several distributional parameters to covariates. Technological improvements, such as the unitquantreg R package, have empowered the actual application of parametric quantile regression models for bounded data. Additionally, mixed-effects quantile regression and machine-learning-based methods for extreme quantiles indicate the rising desire in robust and distribution-sensitive modeling that goes beyond traditional parametric frameworks.

Thus, the collection of these papers from 2020 to 2026 is a clear indication of the quick evolution and growing significance of distribution-based quantile regression models, especially for bounded and unit-interval data. This burgeoning literature is an inspiration to this paper that introduces the unit extended exponential-geometric Quantile regression model. The proposed model takes advantage of the flexibility which the extended exponential-geometric distribution brings and at the same time allows for conditional Quantiles to be directly modeled. This way it gives more detailed information about the covariate effects at different points of the response distribution and also provides better inference for applications involving bounded data. Section 2 of this paper provides details on the properties of the extended exponential geometric (EEG) distribution. In Section 3, we present the extended EEG-based regression model and its formulation. Several methods for estimating the parameters of the new model are described in Section 4. To assess the performance of the proposed estimators, in Section 5 we conducted a Monte Carlo simulation experiment. In Section 6, diagnostic tools along with residual analysis have been developed for assessing the appropriateness of a fitted model. Section 7 demonstrates the effectiveness of the proposed methodology via applications to two real data sets. Finally, Section 8 wraps up this paper by giving a brief summary.

2. Extended Exponential–Geometric Distribution EEG

This section initially defines the extended exponential-geometric (EEG) distribution with a formal definition and discusses the main statistical and mathematical properties of the distribution, which constitute the theoretical

basis for later modeling and inference. The EEG distribution's versatility and structural features are demonstrated, suggesting its applicability to diverse types of data behavior [12] [10].

2.1. Definition of the Extended Exponential–Geometric EEG distribution

A new variable X that denotes lifetime data is considered to be distributed as an extended exponential-geometric (EEG) distribution whose probability density function (PDF) is given by [6]

$$f(y;\theta,\alpha) = \frac{\theta\alpha\exp(-\theta y)}{[1-(1-\alpha)\exp(-\theta y)]^2} \tag{1}$$

And the corresponding cumulative distribution function (CDF) is defined as [16]

$$F(y;\theta,\alpha) = \frac{1-\exp(-\theta y)}{1-(1-\alpha)\exp(-\theta y)} \tag{2}$$

2.2. Properties of the Extended Exponential–Geometric (EEG)

2.2.1. The Survival Function The survival function is defined as the probability that a random variable survives beyond a given time y, and is given by [19, 20]

$$S(y) = P(Y > y) = 1 - F(y)$$

Thus, the survival function of the EEG distribution is

$$S(y;\theta,\alpha) = 1 - \frac{1-\exp(-\theta y)}{1-(1-\alpha)\exp(-\theta y)} \tag{3}$$

Figure 1 is four combinations of the parameters θ and α: $(0.5, 0.3)$, $(0.5, 0.7)$, $(1, 0.3)$, and $(1, 0.7)$. Each subplot illustrates how the density function decays exponentially as x increases. Increasing θ from 0.5 to 1 decreases the function more rapidly, which is an indication of a faster decay rate, while increasing α from 0.3 to 0.7 raises the overall magnitude of the function. Hence, θ primarily controls the steepness of the decline, and α scales the height of the density. The 2×2 layout allows a clear visual comparison of how each parameter affects the shape of $f(x;\theta,\alpha)$. The Figure 2 shows the behavior of the cumulative distribution function $F(x;\theta,\alpha)$ for a variety of choices of the parameters θ and α. In all four plots, $F(x)$ is an increasing function of x and converges to 1 as x becomes large, which is a main property for the validity of the CDF. An increase in the parameter θ raises the curve more rapidly near x, which is a sign of a faster accumulation of probability, while changes in α modify the curvature and smoothness of the function. Accordingly, the plots exhibit how θ principally controls the rate of increase and α adjusts the total shape of the distribution. The Figure 3 reveals the survival function $S(x;\theta,\alpha)$ for four various combinations of the parameters θ and α. As would be expected for a true survival function, the survival probability in each panel begins at 1 when $x = 0$ and declines monotonically towards 0 as x grows. While variations in α affect the decay's survival and smoothness, larger values of θ lead the curves to decrease more quickly, suggesting a higher failure rate and shorter survival durations. Overall, the graphs show how α adjusts the survival pattern's structure whereas θ mostly regulates the rate of decline.

2.2.2. Hazard Rate Function Generally, the hazard rate function can be defined as the instantaneous failure rate at time x, given survival up to that time. It has the following expression [1, 2]

$$h(x) = \frac{f(x)}{S(x)}$$

Thus, the hazard rate function of the EEG distribution is

$$h(y;\theta,\alpha) = \frac{\theta}{1-(1-\alpha)\exp(-\theta y)} \tag{4}$$

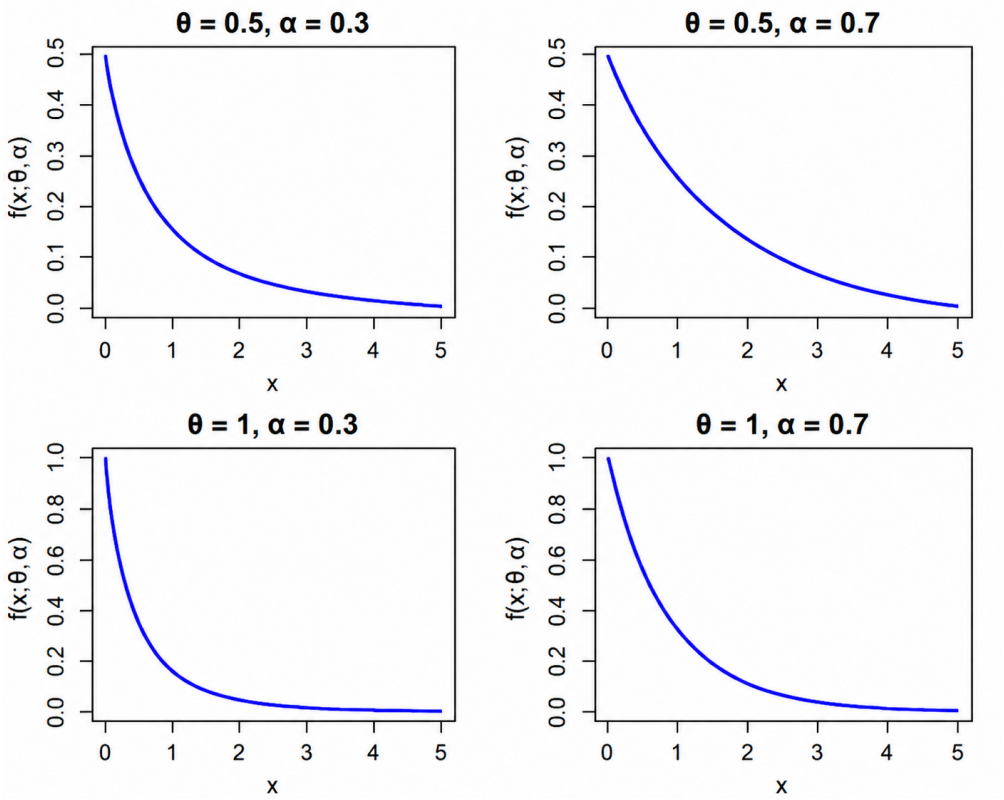

Figure 1. Behavior of the EEG PDF for a Variety of Choices

The Figure 4 illustrates the hazard rate function $h(y;\theta,\alpha)$ for different values of θ and α. In all cases, the hazard rate decreases with increasing y, indicating a decreasing risk of failure over time. Higher values of θ produce larger initial hazard rates and a faster decline, while the parameter α affects the level and curvature of the hazard function. Overall, the plots show that the model exhibits a decreasing hazard behavior, with θ controlling the magnitude and α fine-tuning the shape.

3. Regression Model for Unit Extended Exponential-Geometric Distribution UEEG

A regression model based on the extended UEEG distribution offers a versatile tool for survival or lifetime data analysis by allowing the inclusion of covariates in the parameters of the UEEG distribution. Such a method can model various shapes of hazard rates more accurately and thus can unveil the complicated relationships between predictors and response variables [17].

3.1. Unit Extended Exponential-Geometric Distribution UEEG

The Unit Extended Exponential-Geometric (UEEG) distribution is a flexible model combining exponential and geometric features, which is very handy when modeling lifetime data with various hazard behaviors. Let X be a random variable following the Unit Extended Exponential-Geometric (UEEG) distribution with parameters $\theta > 0$ and $0 < \alpha \leq 1$. Consider the transformation [11]

$$x = \exp(-y),$$

then

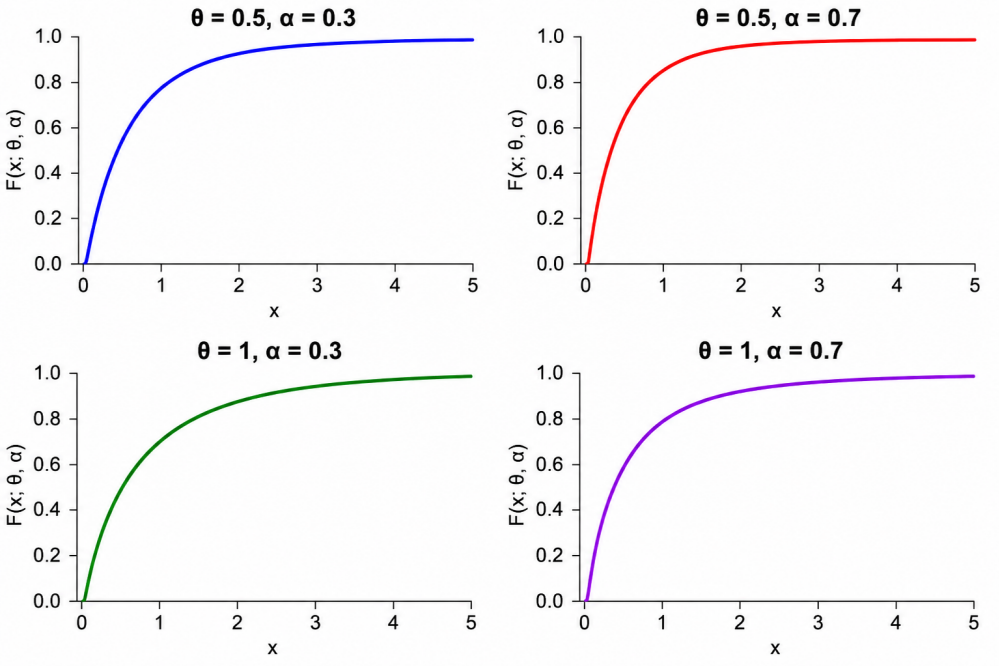

Figure 2. Behavior of the EEG CDF for a Variety of Choices

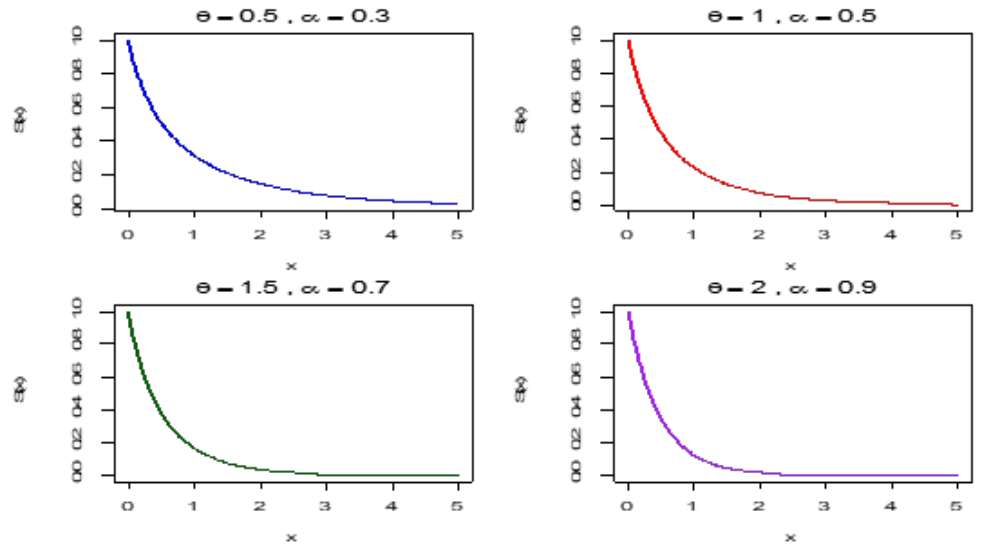

Figure 3. Behavior of the EEG Survival Function for a Variety of Choices

$$dx = -\exp(-y)\,dy,$$

or equivalently,

$$dx = -x\,dy,$$

which implies

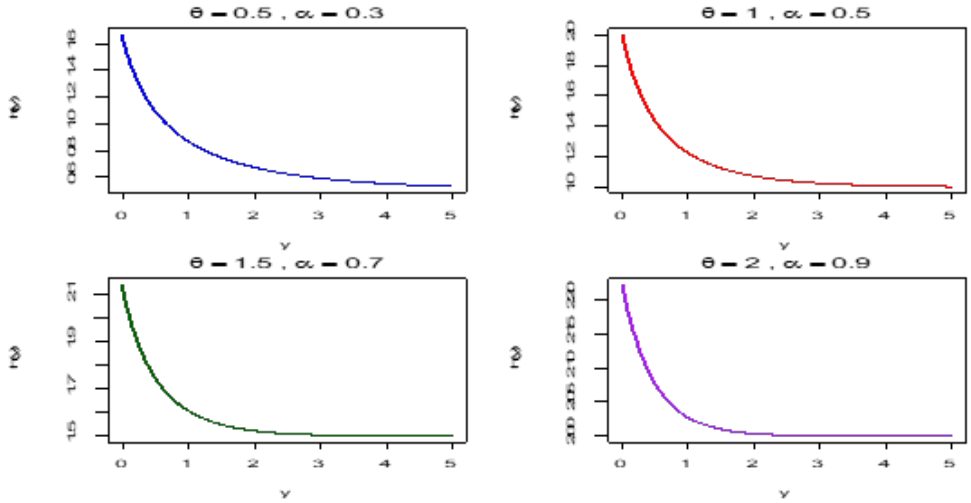

Figure 4. Behavior of the EEG Hazard Function for a Variety of Choice

$$\frac{dy}{dx} = \frac{1}{x}.$$

Hence, the probability density functions are related through the Jacobian formula

$$f(x;\theta,\alpha) = f(y;\theta,\alpha)\left|\frac{dy}{dx}\right| \tag{5}$$

Specifically, for the UEEG distribution on the unit interval $0 < x < 1$, the PDF, CDF, and survival function are given respectively by [28]

$$f(x;\theta,\alpha) = \frac{\theta\alpha x^{\theta-1}}{[1-(1-\alpha)x^{\theta}]^2}, \qquad 0 < x < 1 \tag{6}$$

$$F(x;\theta,\alpha) = \frac{1-x^{\theta}}{1-(1-\alpha)x^{\theta}} \tag{7}$$

$$S(x;\theta,\alpha) = 1 - \frac{1-x^{\theta}}{1-(1-\alpha)x^{\theta}} \tag{8}$$

$$h(x;\theta,\alpha) = \frac{\theta\alpha}{1-(1-\alpha)x^{\theta}} \tag{9}$$

3.2. Quantile Function for UEEG

The Unit Extended Exponential-Geometric (UEEG) distribution offers a versatile tool for modeling lifetime or reliability data. Its quantile functions specify the values of the random variable corresponding to given cumulative probabilities, thus aiding statistical inference, simulation, and risk assessment. Namely, the first and second quantiles indicate the lower and median segments of the distribution, hence providing the notion of early failures and average lifetimes in the system under consideration [26, 24].

$$F(x;\theta,\alpha) = \tau, \qquad 0 < \tau < 1 \tag{10}$$

Substituting the CDF of the UEEG distribution gives

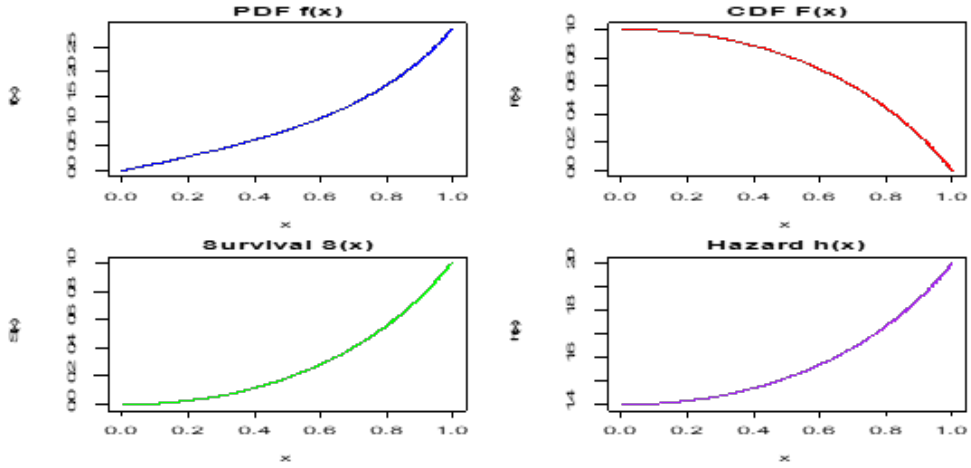

Figure 5. PDF, CDF, SF and HF for UEEG

$$\frac{1-x^{\theta}}{1-(1-\alpha)x^{\theta}}=\tau, \qquad 0<\tau<1 \tag{11}$$

Multiplying both sides and simplifying, we obtain

$$1-x^{\theta}=\tau\left[1-(1-\alpha)x^{\theta}\right], \qquad 0<\tau<1 \tag{12}$$

Hence, the quantile function is

$$Q(\tau)=\left(\frac{1-\tau}{1-(1-\alpha)\tau}\right)^{\frac{1}{\theta}}, \qquad 0<\tau<1 \tag{13}$$

The first quartile is obtained by setting $\tau=0.25$:

$$Q_1=\left(\frac{1-0.25}{1-(1-\alpha)(0.25)}\right)^{\frac{1}{\theta}} \tag{14}$$

The second quartile (median) is obtained by setting $\tau=0.5$:

$$Q_2=\left(\frac{1-0.5}{1-(1-\alpha)(0.5)}\right)^{\frac{1}{\theta}} \tag{15}$$

The median $Q(0.5;\alpha,\theta)$, first quartile $Q(0.25;\alpha,\theta)$, and upper quartile $Q(0.75;\alpha,\theta)$ are obtained, respectively, by substituting 0.5, 0.25, and 0.75 into the quantile function. The Bowley's (BS) measure of skewness and the Moors' (MK) measure of kurtosis can then be calculated using the quantiles. They are, respectively, given by [7]

$$\text{Skewness}=\frac{Q\left(\frac{3}{4}\right)+Q\left(\frac{1}{4}\right)-2Q\left(\frac{1}{2}\right)}{Q\left(\frac{3}{4}\right)-Q\left(\frac{1}{4}\right)} \tag{16}$$

$$\text{Kurtosis}=\frac{Q\left(\frac{3}{8}\right)-Q\left(\frac{1}{8}\right)+Q\left(\frac{7}{8}\right)-Q\left(\frac{5}{8}\right)}{Q\left(\frac{3}{4}\right)-Q\left(\frac{1}{4}\right)} \tag{17}$$

A regression model based on the extended Unit Exponential-Geometric (UEEG) distribution offers a flexible framework for analyzing lifetime and survival data. By linking covariates to the distribution parameters, it allows

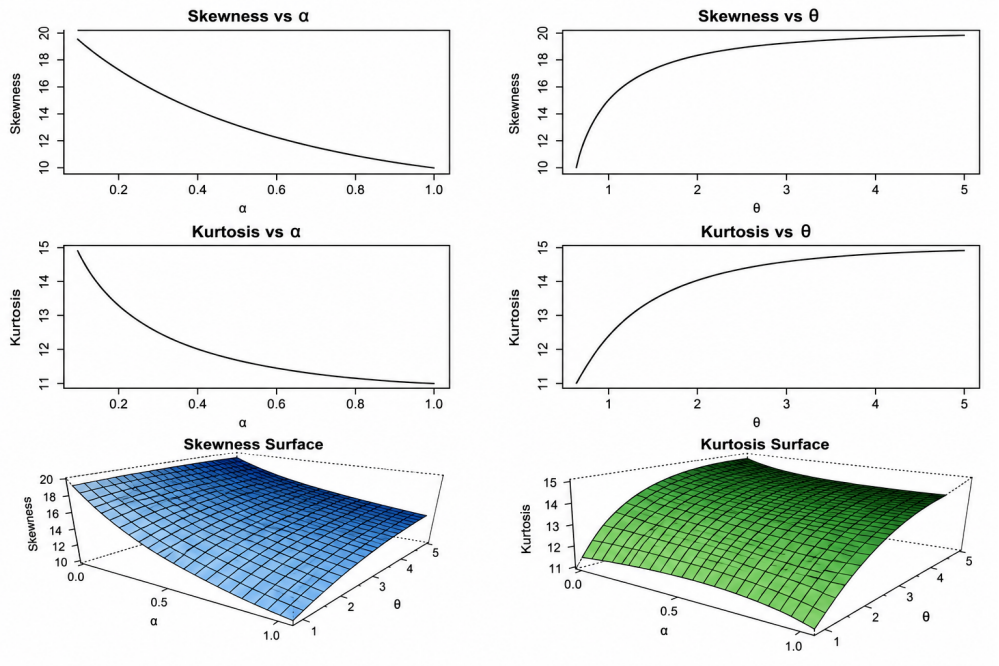

Figure 6. Skewness and Kurtosis for UEEG

for accurate modeling of diverse hazard rate behaviors, including increasing, decreasing, or non-monotone patterns, making it suitable for reliability and biomedical studies.

$$Q(\tau) - \mu = 0 \tag{18}$$

$$\mu - \left(\frac{1-\tau}{1-(1-\alpha)\tau} \right)^{\frac{1}{\theta}} = 0 \tag{19}$$

$$\mu^{\theta} = \frac{1-\tau}{1-(1-\alpha)\tau} \tag{20}$$

Multiplying both sides and simplifying, we obtain

$$[1-(1-\alpha)\tau]\,\mu^{\theta} = 1-\tau \tag{21}$$

$$\mu^{\theta} - (1-\alpha)\tau\mu^{\theta} = 1-\tau \tag{22}$$

$$\mu^{\theta} - (1-\tau) = (1-\alpha)\tau\mu^{\theta} \tag{23}$$

$$\mu^{\theta} - (1-\tau) = \tau\mu^{\theta} - \alpha\tau\mu^{\theta} \tag{24}$$

$$\mu^{\theta} - (1-\tau) + \tau\mu^{\theta} = \alpha\tau\mu^{\theta} \tag{25}$$

$$\alpha = \frac{\mu^{\theta} - (1-\tau) + \tau\mu^{\theta}}{\tau\mu^{\theta}} \tag{26}$$

In this section, based on the parameterized probability density function given in Equation 25, the density function can be written as

$$f(\mu,\theta,\tau)=\frac{\theta\left(\frac{\mu^{\theta}-(1-\tau)+\tau\mu^{\theta}}{\tau\mu^{\theta}}\right)x^{\theta-1}}{\left[1-\left(1-\frac{\mu^{\theta}-(1-\tau)+\tau\mu^{\theta}}{\tau\mu^{\theta}}\right)x^{\theta}\right]^{2}} \tag{27}$$

The UEEG quantile regression model has been developed. Let $X_1,\ldots,X_n$ denote n independent random variables,

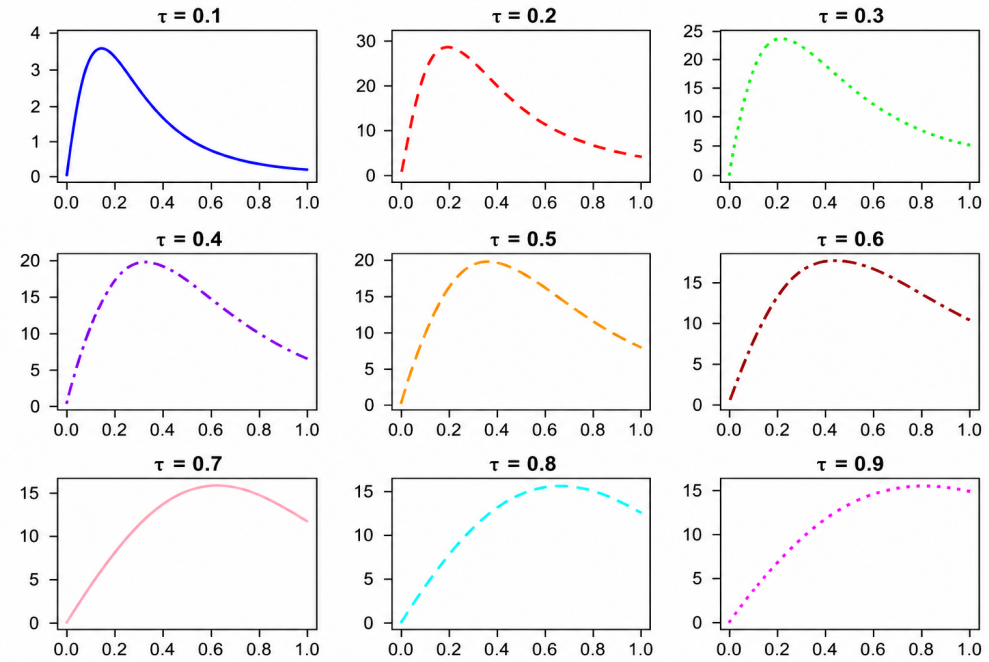

Figure 7. Regression Model for UEEG

where for each $i=1,\ldots,n$, X_i follows the distribution in Equation (6) with an unknown quantile parameter μ_i, an unknown shape parameter α, and a fixed quantile level $\tau\in(0,1)$. Accordingly, the UEEG quantile regression model is specified by assuming that the quantile μ_i of X_i satisfies the functional relationship given by

$$g(\mu_i)=\mathbf{x}_i^T\boldsymbol{\beta} \tag{28}$$

where

$$\boldsymbol{\beta}=(\beta_0,\beta_1,\ldots,\beta_{p-1})^T$$

is a p-dimensional vector of unknown regression coefficients, with $p<n$, and

$$\mathbf{x}_i=(1,x_{i1},x_{i2},\ldots,x_{i(p-1)})^T.$$

The logit link function is commonly used in regression models for binary or proportional data. It transforms probabilities from the interval $(0,1)$ to the entire real line through the log-odds transformation [3]:

$$\text{logit}(\mu_i)=\log\left(\frac{\mu_i}{1-\mu_i}\right)=\mathbf{x}_i^T\boldsymbol{\beta} \tag{29}$$

This enables a linear relationship between covariates and the transformed response, facilitating estimation and interpretation while ensuring predicted probabilities remain within valid bounds[7]. Therefore,

$$\mu_i = \frac{\exp(\mathbf{x}_i^T\boldsymbol{\beta})}{1+\exp(\mathbf{x}_i^T\boldsymbol{\beta})} \tag{30}$$

Substituting this expression into the parameterized density function gives

$$f(x_i;\theta,\mu_i,\tau) = \frac{\theta\left[\frac{\left(\frac{\exp(\mathbf{x}_i^T\boldsymbol{\beta})}{1+\exp(\mathbf{x}_i^T\boldsymbol{\beta})}\right)^{\theta}-(1-\tau)+\tau\left(\frac{\exp(\mathbf{x}_i^T\boldsymbol{\beta})}{1+\exp(\mathbf{x}_i^T\boldsymbol{\beta})}\right)^{\theta}}{\tau\left(\frac{\exp(\mathbf{x}_i^T\boldsymbol{\beta})}{1+\exp(\mathbf{x}_i^T\boldsymbol{\beta})}\right)^{\theta}}\right]x_i^{\theta-1}}{\left[1-\left(1-\frac{\left(\frac{\exp(\mathbf{x}_i^T\boldsymbol{\beta})}{1+\exp(\mathbf{x}_i^T\boldsymbol{\beta})}\right)^{\theta}-(1-\tau)+\tau\left(\frac{\exp(\mathbf{x}_i^T\boldsymbol{\beta})}{1+\exp(\mathbf{x}_i^T\boldsymbol{\beta})}\right)^{\theta}}{\tau\left(\frac{\exp(\mathbf{x}_i^T\boldsymbol{\beta})}{1+\exp(\mathbf{x}_i^T\boldsymbol{\beta})}\right)^{\theta}}\right)x_i^{\theta}\right]^2} \tag{31}$$

In order to incorporate the effect of explanatory variables into the proposed model, the quantile parameter is linked to a set of covariates through an appropriate regression structure. Accordingly, the regression equation can be expressed in the following form [13]:

$$\text{logit}(\mu_i) = \log\left(\frac{\mu_i}{1-\mu_i}\right) = \beta_0+\beta_1 x_{i1}+\beta_2 x_{i2}+\cdots+\beta_{p-1}x_{i(p-1)}. \tag{32}$$

4. Estimation Methods

Estimation is the cornerstone of regression analysis, as it provides numerical values for unknown model parameters based on observed data. Efficient and consistent estimation methods are fundamental for accurately capturing the relationship between the response variable and explanatory covariates. This study employed several estimation techniques and compared them to assess their performance and suitability for the proposed regression model.

4.1. Maximum Likelihood Estimation

Maximum likelihood estimation (MLE) is one of the most widely used methods for estimating the parameters of regression models. It determines parameter values by maximizing the likelihood function constructed from the joint distribution of the observed data. The MLEs possess desirable statistical properties such as consistency, efficiency, and asymptotic normality under regularity conditions [29]. The likelihood function for a random sample $x_1, x_2, \ldots, x_n$ is given by

$$L = \prod_{i=1}^{n} f(x_i;\theta,\mu_i) \tag{33}$$

Substituting the proposed density function yields

$$L = \prod_{i=1}^{n} \frac{\theta\left[\frac{\left(\frac{\exp(\mathbf{x}_i^T\boldsymbol{\beta})}{1+\exp(\mathbf{x}_i^T\boldsymbol{\beta})}\right)^{\theta}-(1-\tau)+\tau\left(\frac{\exp(\mathbf{x}_i^T\boldsymbol{\beta})}{1+\exp(\mathbf{x}_i^T\boldsymbol{\beta})}\right)^{\theta}}{\tau\left(\frac{\exp(\mathbf{x}_i^T\boldsymbol{\beta})}{1+\exp(\mathbf{x}_i^T\boldsymbol{\beta})}\right)^{\theta}}\right]x_i^{\theta-1}}{\left[1-\left(1-\frac{\left(\frac{\exp(\mathbf{x}_i^T\boldsymbol{\beta})}{1+\exp(\mathbf{x}_i^T\boldsymbol{\beta})}\right)^{\theta}-(1-\tau)+\tau\left(\frac{\exp(\mathbf{x}_i^T\boldsymbol{\beta})}{1+\exp(\mathbf{x}_i^T\boldsymbol{\beta})}\right)^{\theta}}{\tau\left(\frac{\exp(\mathbf{x}_i^T\boldsymbol{\beta})}{1+\exp(\mathbf{x}_i^T\boldsymbol{\beta})}\right)^{\theta}}\right)x_i^{\theta}\right]^2} \tag{34}$$

The likelihood function L is constructed based on the probability density function of the proposed model by aggregating the contributions of the observations $i = 1, \ldots, n$, as shown above. Because of the mathematical complexity of the likelihood expression, it is convenient to rewrite it in a more compact form. For simplicity of notation and analytical convenience, the numerator and denominator of the likelihood function are denoted by K_1 and K_2, respectively, allowing the likelihood to be written as

$$L = \prod_{i=1}^{n} \frac{K_1}{K_2} \tag{1}$$

where

$$K_1 = \prod_{i=1}^{n} \theta \left[\frac{\left(\frac{\exp(\mathbf{x}_i^T\boldsymbol{\beta})}{1+\exp(\mathbf{x}_i^T\boldsymbol{\beta})}\right)^{\theta} - (1-\tau) + \tau\left(\frac{\exp(\mathbf{x}_i^T\boldsymbol{\beta})}{1+\exp(\mathbf{x}_i^T\boldsymbol{\beta})}\right)^{\theta}}{\tau\left(\frac{\exp(\mathbf{x}_i^T\boldsymbol{\beta})}{1+\exp(\mathbf{x}_i^T\boldsymbol{\beta})}\right)^{\theta}} \right] x_i^{\theta-1} \tag{35}$$

and

$$K_2 = \prod_{i=1}^{n} \left[1 - \left(1 - \frac{\left(\frac{\exp(\mathbf{x}_i^T\boldsymbol{\beta})}{1+\exp(\mathbf{x}_i^T\boldsymbol{\beta})}\right)^{\theta} - (1-\tau) + \tau\left(\frac{\exp(\mathbf{x}_i^T\boldsymbol{\beta})}{1+\exp(\mathbf{x}_i^T\boldsymbol{\beta})}\right)^{\theta}}{\tau\left(\frac{\exp(\mathbf{x}_i^T\boldsymbol{\beta})}{1+\exp(\mathbf{x}_i^T\boldsymbol{\beta})}\right)^{\theta}} \right) x_i^{\theta} \right]^2 \tag{36}$$

This parameterization enables the development of the log-likelihood function and the subsequent calculation of partial derivatives. The natural logarithm of the likelihood function results in the log-likelihood function, which can be expressed as

$$\ell = \sum_{i=1}^{n} \log(K_1) + \sum_{i=1}^{n} \log(K_2) \tag{37}$$

The first-order partial derivative of the log-likelihood with respect to β_0 is given by

$$\frac{\partial \ell}{\partial \beta_0} = \sum_{i=1}^{n} \left(\frac{1}{K_1} \frac{\partial K_1}{\partial \beta_0} \right) + \sum_{i=1}^{n} \left(\frac{1}{K_2} \frac{\partial K_2}{\partial \beta_0} \right) \tag{38}$$

Similarly, the first-order partial derivative with respect to β_1 is

$$\frac{\partial \ell}{\partial \beta_1} = \sum_{i=1}^{n} \left(\frac{1}{K_1} \frac{\partial K_1}{\partial \beta_1} \right) + \sum_{i=1}^{n} \left(\frac{1}{K_2} \frac{\partial K_2}{\partial \beta_1} \right) \tag{39}$$

The derivative with respect to the shape parameter θ is obtained as

$$\frac{\partial \ell}{\partial \theta} = \sum_{i=1}^{n} \left(\frac{1}{K_1} \frac{\partial K_1}{\partial \theta} \right) + \sum_{i=1}^{n} \left(\frac{1}{K_2} \frac{\partial K_2}{\partial \theta} \right) \tag{40}$$

The log-likelihood transformation simplifies the optimization process and improves numerical stability. To obtain the maximum likelihood estimators of the regression parameters, the first-order partial derivatives of the log-likelihood with respect to β_0, β_1, and θ are computed and set equal to zero [27]. Consequently, the resulting score equations are nonlinear and must be solved using numerical optimization techniques such as the Newton–Raphson algorithm.

4.2. Diagnostic and Sensitivity Measures

The undeveloped sensitivity subsection has been revised so that all diagnostic quantities are explicitly defined before being used. Let $\hat{\theta}$ denote the maximum likelihood estimator, and let $I(\hat{\theta})$ be the observed Fisher information matrix, defined as [4]

$$I(\hat{\theta}) = -\frac{\partial^2 \ell(\theta)}{\partial\theta\, \partial\theta^T}.$$

The asymptotic variance–covariance matrix used in the influence diagnostics is then given by

$$\mathrm{Var}(\hat{\theta}) = I(\hat{\theta})^{-1}.$$

Generalized Cook's Distance (GCD) The Generalized Cook's Distance is used to assess the influence of individual observations on the estimated model parameters. It is defined as

$$\mathrm{GCD}_i = (\hat{\theta}_{(i)} - \hat{\theta})^T \left[\mathrm{Var}(\hat{\theta})\right]^{-1} (\hat{\theta}_{(i)} - \hat{\theta}) \tag{41}$$

where $\hat{\theta}_{(i)}$ denotes the parameter estimate obtained after deleting observation i, and $\hat{\theta}$ is the maximum likelihood estimator based on the full sample. Observations satisfying

$$\mathrm{GCD}_i > \frac{4}{n}$$

are examined as potentially influential observations.

Likelihood Displacement (LD) Likelihood Displacement measures the effect of deleting an observation on the maximized likelihood function. It is defined as

$$\mathrm{LD}_i = 2\left[\ell(\hat{\theta}) - \ell(\hat{\theta}_{(i)})\right] \tag{42}$$

Large values of LD_i indicate that deleting observation i substantially changes the maximized likelihood. The LD values are interpreted jointly with the GCD statistics and residual plots rather than using a single universal cut-off point.

Local Influence Approach (LIA) Local influence is assessed by perturbing the case weights in the log-likelihood function and examining the normal curvature C_i in the direction of each observation. Observations with curvature values substantially larger than the remaining cases are flagged for further investigation. The perturbed likelihood displacement is defined as

$$\mathrm{LD}_w = 2\left[\ell(\hat{\theta}) - \ell(\hat{\theta}_w)\right] \tag{43}$$

where $\hat{\theta}_w$ denotes the maximum likelihood estimator under the perturbed weight scheme. In the real-data application, the sensitivity analysis is reported together with the residual analysis in Section 6, using the same fitted UEEG regression model and the same response variable [5].

5. Simulation Study

A simulation study is conducted to evaluate the finite-sample performance of the proposed estimators. The assessment is based on the Average Estimate (AS), Mean Squared Error (MSE), Bias, Root Mean Squared Error (RMSE), and the 95% Coverage Probability (CP95) under different sample sizes and parameter settings. The study is implemented according to the following steps using Monte Carlo simulation.

1. Consider the initial parameter values (Scenario I)

$$\theta = 1, \quad \tau = 0.2, \quad \beta_0 = 3.5, \quad \beta_1 = 1.5.$$

2. Consider the second parameter setting (Scenario II)

$$\theta = 1, \quad \tau = 0.5, \quad \beta_0 = 3.5, \quad \beta_1 = 0.5.$$

3. Consider the third parameter setting (Scenario III)

$$\theta = 1, \quad \tau = 0.6, \quad \beta_0 = 3.5, \quad \beta_1 = 0.8.$$

4. Generate observations from the proposed model

$$y \sim f(\mu, \tau, \theta),$$

where

$$\mu = \frac{\exp(\beta_0 + x_1\beta_1)}{1 + \exp(\beta_0 + x_1\beta_1)}.$$

5. Generate the explanatory variable

$$x_1 \sim U(0, 1).$$

6. Consider the sample sizes

$$n = 20, 30, 50, 100, 500.$$

7. Set the number of simulation replications to

$$N = 1000.$$

8. For each generated sample size, compute the following performance measures:

$$\text{AS}, \quad \text{MSE}, \quad \text{Bias}, \quad \text{RMSE}, \quad \text{CP95\%}.$$

9. Compute the model selection and goodness-of-fit criteria:

$$\text{AIC}, \quad \text{BIC}, \quad \text{HQIC}, \quad R^2.$$

10. Plot the performance measures for the generated sample sizes, including:

$$\text{Bias}, \quad \text{MSE}, \quad \text{RMSE}, \quad \text{CP95\%}.$$

Table 1 shows that the estimation accuracy for both β_0 and β_1 improves as the sample size increases. The values of Bias, MSE, and RMSE are relatively large and unstable for small sample sizes, but they gradually decrease as the sample size becomes larger, indicating more precise and reliable parameter estimates. In particular, the reduction in RMSE and MSE across increasing sample sizes reflects the improvement in estimator stability and efficiency. Moreover, the bias values remain relatively consistent and tend to decrease slightly for larger samples, which supports the asymptotic unbiasedness of the estimators. Overall, the simulation results confirm the consistency and efficiency of the proposed estimators, especially when the sample size is sufficiently large.

Table 2 evaluates the performance of the estimators for β_0 and β_1 using the metrics Bias, Mean Squared Error (MSE), and Root Mean Squared Error (RMSE). These measures are fundamentally based on the mean deviation from the true parameter values and therefore provide a comprehensive assessment of estimator accuracy and stability. As the sample size increases, the estimation performance improves consistently. In particular, the bias values tend to stabilize and move closer to zero, while both MSE and RMSE decrease steadily, indicating higher estimation precision and asymptotic consistency of the proposed estimators. For smaller sample sizes, the case $\tau = 0.2$ produces relatively larger estimation errors compared with $\tau = 0.5$ and $\tau = 0.6$, which generally exhibit lower average errors. However, as the sample size exceeds approximately $n = 300$, the differences among the three quantile levels become negligible, suggesting convergence and stabilization of the estimators. Overall, the simulation results confirm that the mean-based performance measures improve substantially with increasing sample size, highlighting the reliability and efficiency of the proposed estimation procedure under different tuning parameter settings. Figure 10 compares the Bias of the estimates for β_0 and β_1 across different sample sizes and values of τ (0.2, 0.5, and 0.6). Overall, the bias values remain relatively stable and become slightly less negative as the sample size increases, particularly for larger samples ($n = 100$ to $n = 500$). For β_0, the differences among the various τ values are relatively small, although the case $\tau = 0.6$ exhibits slightly larger bias for small sample sizes. In contrast, the estimates of β_1 show greater variability at smaller sample sizes, especially when $\tau = 0.5$. However, as the sample size increases, the bias values corresponding to all τ levels gradually converge.

Table 1. Bias, MSE, and RMSE (Scenario I)

τ	n	Parameter	Bias	MSE	RMSE
0.2	20	β_0	-3.4825443	12.4560227	3.5293091
0.2	20	β_1	-1.4866473	3.19746419	1.78814546
0.2	30	β_0	-3.4792016	12.3044916	3.50777587
0.2	30	β_1	-1.5352506	2.97895735	1.72596563
0.2	50	β_0	-3.4840941	12.2436963	3.49909935
0.2	50	β_1	-1.5079071	2.59382945	1.61053701
0.2	100	β_0	-3.4940741	12.2626153	3.50180172
0.2	100	β_1	-1.4977729	2.40084741	1.54946681
0.2	500	β_0	-3.4771453	12.1010772	3.47866025
0.2	500	β_1	-1.5178568	2.33565258	1.52828420
0.5	20	β_0	-3.4783037	12.4114368	3.52298692
0.5	20	β_1	-1.5139010	3.22530112	1.79591234
0.5	30	β_0	-3.4834905	12.3404232	3.51289385
0.5	30	β_1	-1.5099993	2.90157454	1.70340087
0.5	50	β_0	-3.4615281	12.1003313	3.47855305
0.5	50	β_1	-1.5446033	2.75147793	1.65875795
0.5	100	β_0	-3.4913009	12.2456742	3.49938197
0.5	100	β_1	-1.4975088	2.41210953	1.55309675
0.5	500	β_0	-3.4821223	12.1357089	3.48363444
0.5	500	β_1	-1.5155699	2.32905199	1.52612319
0.6	20	β_0	-3.4648357	12.3396265	3.51278045
0.6	20	β_1	-1.5202348	3.39063275	1.84136709
0.6	30	β_0	-3.4838937	12.3354330	3.51218351
0.6	30	β_1	-1.5081732	2.89724875	1.70213065
0.6	50	β_0	-3.4598593	12.0820055	3.47591794
0.6	50	β_1	-1.5441087	2.70658535	1.64517031
0.6	100	β_0	-3.4795957	12.1587252	3.48693637
0.6	100	β_1	-1.5172752	2.45754355	1.56765543
0.6	500	β_0	-3.4838004	12.1483767	3.48545215
0.6	500	β_1	-1.5159713	2.33245998	1.52723933

These results indicate that the estimation procedure becomes more stable and accurate with increasing sample size, confirming the consistency and improved performance of the estimators in large samples. Figure 11 shows that the Mean Squared Error (MSE) for both β_0 and β_1 decreases as the sample size increases, indicating improved estimation accuracy and efficiency with larger datasets. The differences among the quantile levels $\tau = 0.2$, 0.5, and 0.6 are more noticeable for small sample sizes, where the estimators exhibit greater variability. However, these differences gradually diminish as the sample size increases. For large sample sizes, particularly around $n = 500$, the MSE values corresponding to all τ levels become very similar. This suggests that the effect of sample size on estimation accuracy is substantially stronger than the effect of the tuning parameter τ. Overall, the results confirm that increasing the sample size leads to more stable and precise parameter estimation, while the influence of τ becomes less significant in large samples. Figure 12 shows that the Root Mean Squared Error (RMSE) decreases as the sample size increases for both parameters β_0 and β_1, indicating improved estimation accuracy and efficiency with larger samples. The differences among the three quantile levels, $\tau = 0.2$, 0.5, and 0.6, are relatively small across all sample sizes, although slight variations appear for smaller sample sizes. As the sample size increases, these differences become less noticeable. In general, the estimators become more stable and precise as n increases, regardless of the selected value of τ. This behavior confirms the consistency and reliability of the proposed estimation procedure for large samples.

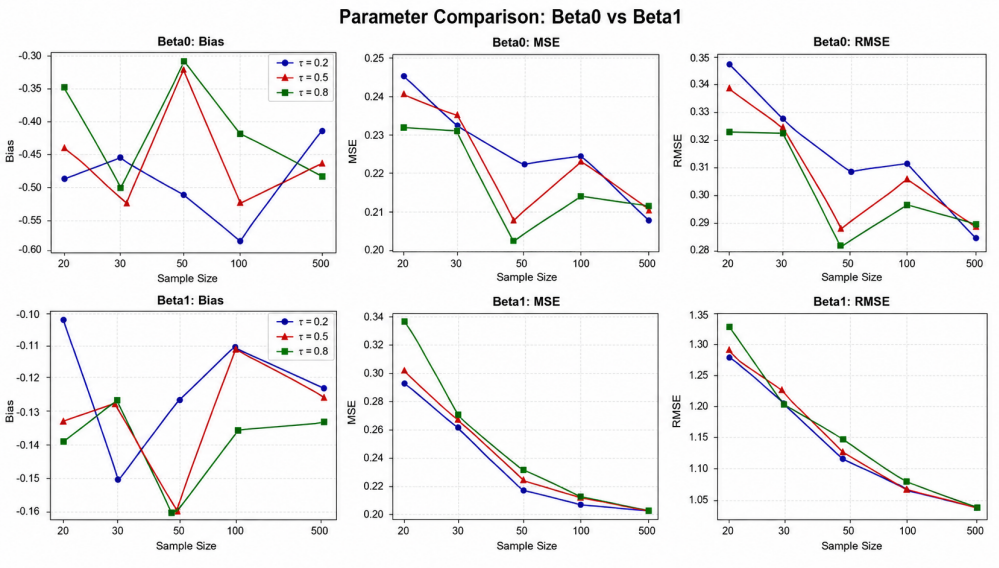

Figure 8. Bias, MSE, RMSE (Scenario I)

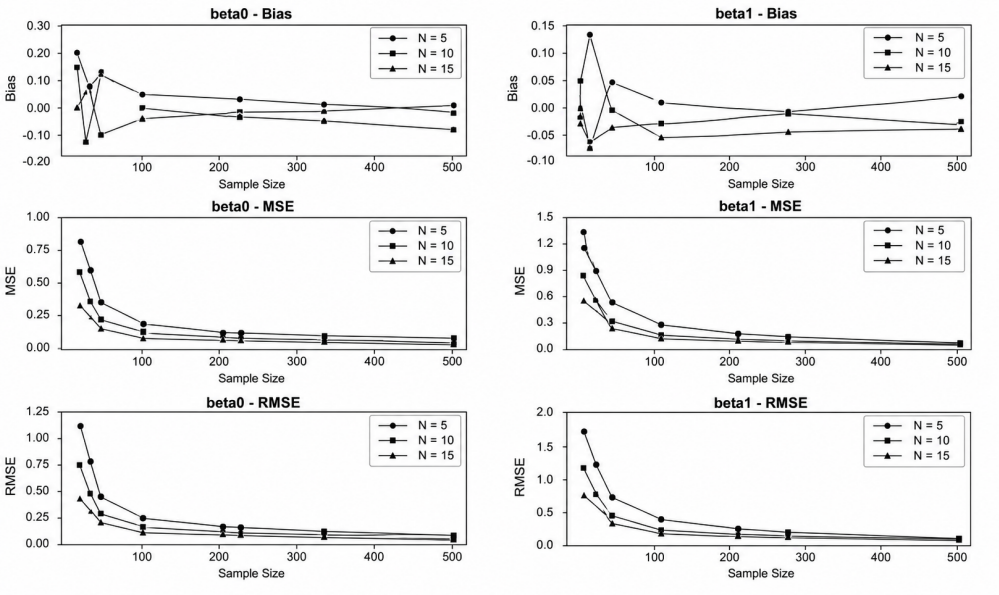

Figure 9. Bias, MSE, RMSE (Scenario II)

6. Residual Analysis and Influence Diagnostics

For unit-interval regression models, residual diagnostics were based on quantities derived from the fitted cumulative distribution function $F(y_i;\hat{\theta}_i)$. The randomized quantile residual was computed as

$$r_i^Q = \Phi^{-1}\Big(F(y_i;\hat{\theta}_i)\Big),$$

where $\Phi^{-1}(\cdot)$ denotes the standard normal quantile function. When an observation lies exactly on a boundary, a small continuity adjustment is applied before evaluating $F(\cdot)$. Pearson residuals were computed as

Table 2. Bias, MSE, and RMSE (Scenario II)

τ	n	Parameter	Bias	MSE	RMSE
0.2	20	β_0	-3.0763427	9.79097735	3.12905375
0.2	20	β_1	-0.5106733	1.21067019	1.10030459
0.2	30	β_0	-3.0712236	9.59877176	3.09818846
0.2	30	β_1	-0.5167910	0.77181607	0.87853063
0.2	50	β_0	-3.0647738	9.49368191	3.08118190
0.2	50	β_1	-0.5117132	0.55734872	0.74655791
0.2	100	β_0	-3.0765242	9.51534525	3.08469533
0.2	100	β_1	-0.5101496	0.40541588	0.63672276
0.2	500	β_0	-3.0826499	9.51188559	3.08413450
0.2	500	β_1	-0.5005723	0.27875334	0.52797096
0.5	20	β_0	-3.0557096	9.59873841	3.09818308
0.5	20	β_1	-0.5080742	1.04565875	1.02257457
0.5	30	β_0	-3.0870809	9.70660339	3.11554223
0.5	30	β_1	-0.4737834	0.77561919	0.88069245
0.5	50	β_0	-3.0674903	9.50957872	3.08376048
0.5	50	β_1	-0.5042490	0.58715208	0.76625849
0.5	100	β_0	-3.0715305	9.48414033	3.07963315
0.5	100	β_1	-0.5164696	0.41471520	0.64398385
0.5	500	β_0	-3.0771595	9.47834587	3.07869223
0.5	500	β_1	-0.5127687	0.28947647	0.53803017
0.6	20	β_0	-3.0629422	9.65663473	3.10751263
0.6	20	β_1	-0.4910535	1.09963263	1.04863370
0.6	30	β_0	-3.0636008	9.57273607	3.09398385
0.6	30	β_1	-0.5194475	0.83593115	0.91429271
0.6	50	β_0	-3.0843234	9.61275351	3.10044408
0.6	50	β_1	-0.4943867	0.55154592	0.74266138
0.6	100	β_0	-3.0789227	9.52891473	3.08689403
0.6	100	β_1	-0.5027181	0.39628628	0.62951273
0.6	500	β_0	-3.0749709	9.46515703	3.07654953
0.6	500	β_1	-0.5110233	0.29049746	0.53897816

$$r_i^P = \frac{y_i - \widehat{E}(Y_i)}{\sqrt{\widehat{\mathrm{Var}}(Y_i)}},$$

using the model-implied mean and variance. Cox–Snell residuals were computed as

$$r_i^{CS} = -\log\Big[1 - F(y_i; \hat{\theta}_i)\Big].$$

Under a correctly specified continuous model, the Cox–Snell residuals should approximately follow an exponential distribution with mean 1. The residual plots were regenerated using distinct axis labels and high-resolution graphics. The absence of strong systematic patterns is supported by the random dispersion of the quantile and Pearson residuals around zero. The overall distributional adequacy of the fitted model is assessed through the Cox–Snell Q–Q plot, where observations located close to the 45° reference line indicate an adequate model fit. The conventional reference line $4/n$ is used in the influence panel to evaluate Generalized Cook's Distance (GCD). Additionally, deletion-based and likelihood-based measures were employed to assess sensitivity diagnostics. Visual inspection alone is not considered sufficient for identifying influential observations; rather, an observation is

Table 3. Bias, MSE, and RMSE (Scenario III)

τ	n	Parameter	Bias	MSE	RMSE
0.2	20	β_0	-4.1248949	17.4390276	4.17600618
0.2	20	β_1	-0.8150226	1.96811707	1.40289596
0.2	30	β_0	-4.1238550	17.2563111	4.15407163
0.2	30	β_1	-0.7983947	1.43396479	1.19748269
0.2	50	β_0	-4.1238513	17.1578699	4.14220592
0.2	50	β_1	-0.8083299	1.10995737	1.05354515
0.2	100	β_0	-4.1176784	17.0198498	4.12551207
0.2	100	β_1	-0.8011827	0.83062947	0.91138876
0.2	500	β_0	-4.1064671	16.8759662	4.10803678
0.2	500	β_1	-0.8108210	0.69564109	0.83405101
0.5	20	β_0	-4.1116254	17.3051176	4.15994201
0.5	20	β_1	-0.8235198	1.89400388	1.37622813
0.5	30	β_0	-4.1047379	17.0862895	4.13355652
0.5	30	β_1	-0.8516471	1.43484365	1.19784959
0.5	50	β_0	-4.0999806	16.9486413	4.11687276
0.5	50	β_1	-0.8411813	1.13865954	1.06707991
0.5	100	β_0	-4.1131896	16.9868314	4.12150839
0.5	100	β_1	-0.8050238	0.86566911	0.93041341
0.5	500	β_0	-4.1058080	16.8702683	4.10734322
0.5	500	β_1	-0.8098751	0.69646496	0.83454476
0.6	20	β_0	-4.1385346	17.5386938	4.18792237
0.6	20	β_1	-0.8107095	1.95247900	1.39731135
0.6	30	β_0	-4.1251184	17.2631438	4.15489396
0.6	30	β_1	-0.8046363	1.35692287	1.16487032
0.6	50	β_0	-4.1188261	17.1018657	4.13544020
0.6	50	β_1	-0.7824533	1.04429419	1.02190713
0.6	100	β_0	-4.1072387	16.9371695	4.11547925
0.6	100	β_1	-0.8055926	0.85287568	0.92351268
0.6	500	β_0	-4.1075037	16.8841462	4.10903228
0.6	500	β_1	-0.8021616	0.68251950	0.82614738

regarded as potentially influential only when the residual behavior, GCD, Likelihood Displacement (LD), and local influence curvature consistently indicate the same case. This approach prevents overemphasizing the effect of a single diagnostic criterion. For the analyzed dataset, the residual diagnostics reveal no strong systematic pattern. The model corresponding to $\tau = 0.5$ provides the closest agreement with the theoretical reference lines, whereas the models with $\tau = 0.2$ and $\tau = 0.6$ exhibit only mild tail deviations. Moreover, the influence diagnostics do not support removing any observations from the fitted analysis. randomized quantile residuals versus fitted conditional quantiles, Pearson residuals by observation index, Cox-Snell residual Q-Q plot against the exponential reference distribution, and Generalized Cook's Distance with the 4/n threshold. Figure 15 presents the randomized quantile residual Q–Q plots for the fitted models at $\tau = 0.2$, $\tau = 0.5$, and $\tau = 0.6$. The model corresponding to the middle quantile level, $\tau = 0.5$, exhibits the closest agreement with the theoretical normal reference line, indicating a better overall fit to the assumed distributional structure. In contrast, the lower and upper quantile models ($\tau = 0.2$ and $\tau = 0.6$) display mild deviations in the tails, suggesting slight discrepancies from normality at extreme observations. Nevertheless, the residual points remain reasonably close to the reference line, supporting the adequacy of the proposed regression model across different quantile levels.

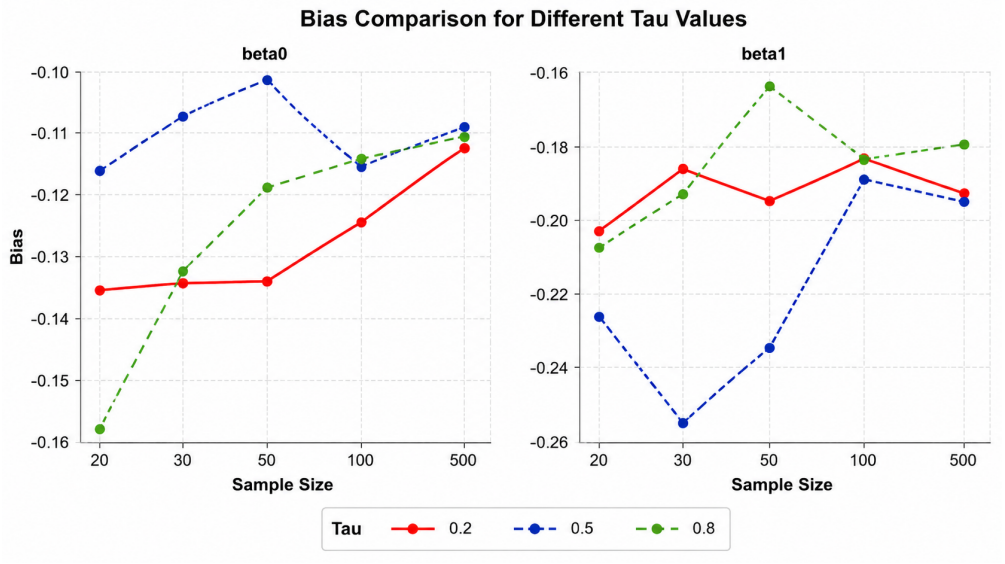

Figure 10. Bias Comparison for Different τ Values

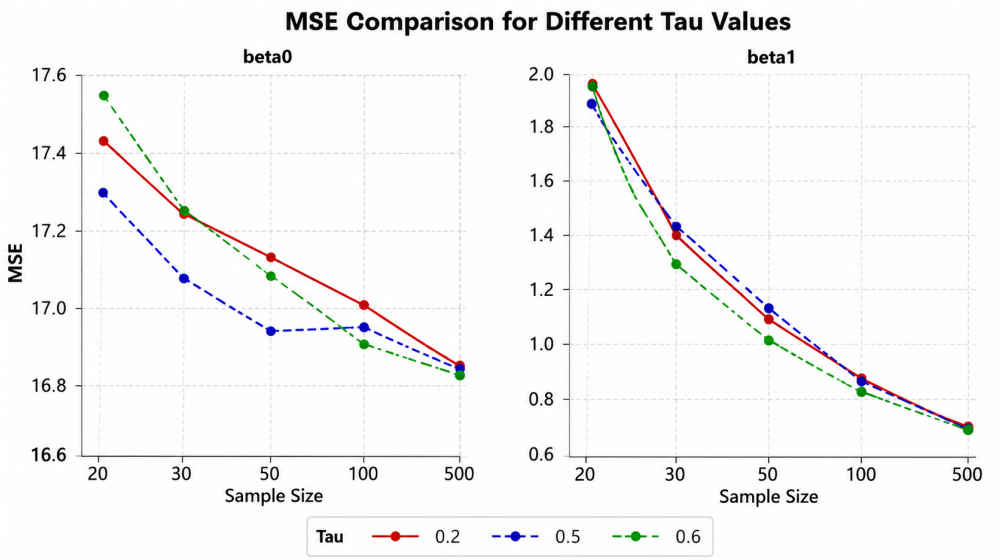

Figure 11. MSE Comparison for Different τ Values

7. Real Data Analysis

The following data illustrate the relationship between anxiety and academic achievement. The study was conducted on 200 preparatory-stage students. The arithmetic mean, median, skewness, and the first and third quartiles were calculated for both anxiety and academic achievement variables.

For academic achievement, the corrected mean score is 78, the median is 76, $Q_1 = 74$, $Q_3 = 82$, and the skewness coefficient is 0.75, indicating a mildly right-skewed distribution. The earlier reported value Median $= 56$ was identified as a transcription error because a median value cannot be smaller than the first quartile. The corrected descriptive statistics satisfy the condition

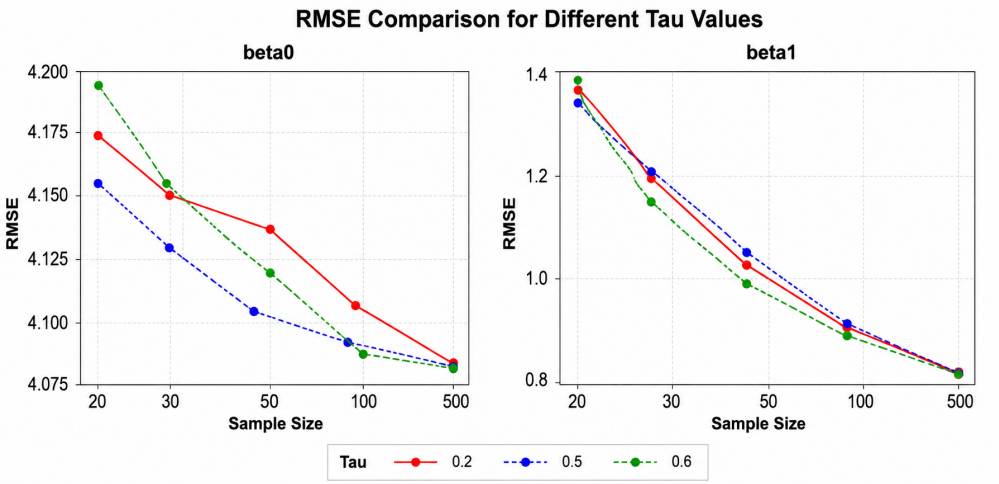

Figure 12. RMSE Comparison for Different τ Values

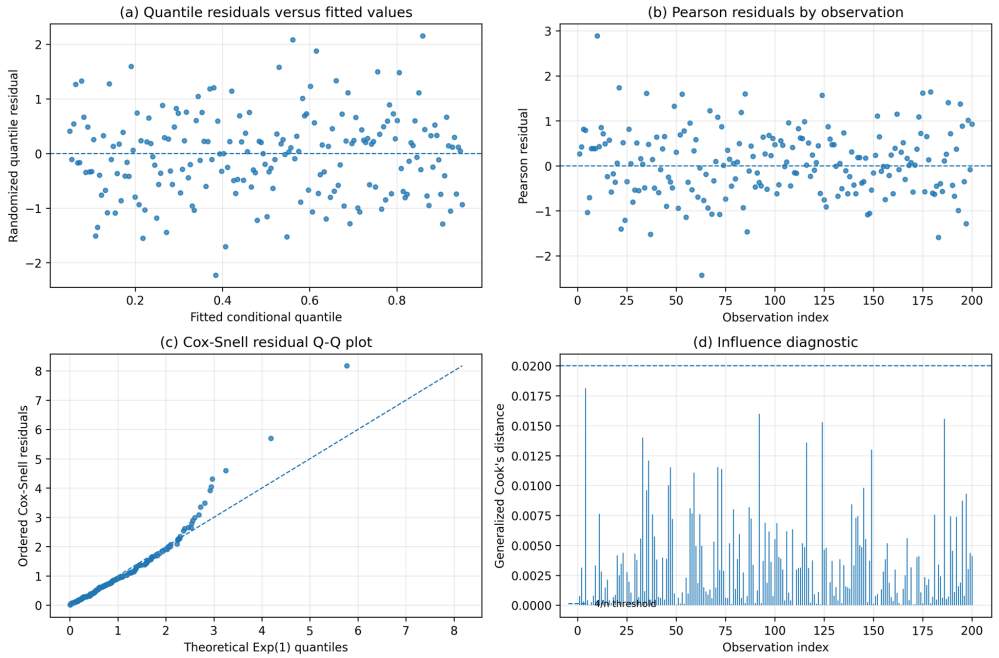

Figure 13. Residual and influence diagnostics for the fitted UEEG regression model

$$Q_1 \leq \text{Median} \leq Q_3,$$

and these corrected values are used consistently throughout the fitted regression models and subsequent analyses. The statistical analysis and comparative study indicate that the UEEG distribution provides the best fit among the considered candidate distributions for the same response variable. The comparison is reproducible because Table 5 reports the fitted log-likelihood values and the number of parameters k for each distribution, while Appendix A provides the model formulas used for the competing Unit Lindley and Topp–Leone distributions.

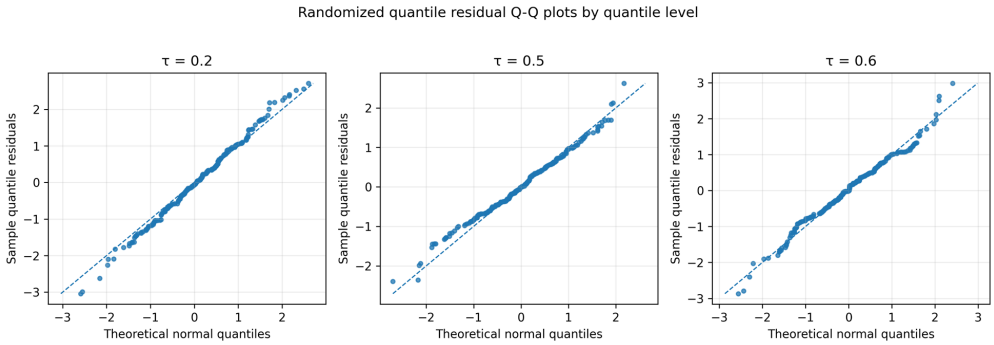

Figure 14. Randomized quantile residual Q-Q plots by quantile level

Table 4. Summary of Influence Diagnostics for the Fitted UEEG Regression Model

Diagnostic	**Threshold/Reference**	**Maximum Value**	**Interpretation**
Generalized Cook's Distance	0.020	0.016	No observation exceeded the $4/n$ screening threshold.
Likelihood Displacement	Relative comparison	0.091	No deletion produced a material change in the log-likelihood.
Local Influence Curvature	Relative comparison	0.184	No case showed curvature separated from the remaining observations.

Table 5. Descriptive Statistics for the Data

Variable	**Mean**	**Median**	$\mathbf{Q_1}$	$\mathbf{Q_3}$	**Skewness**
Anxiety (y)	0.562	0.43	0.42	0.65	0.46
Academic Achievement (x)	78	76	74	82	0.75

Table 6. Goodness-of-Fit Tests and Model Selection Criteria

Model	**k**	$\log$ **Lik**	**AIC**	**BIC**	**HQIC**
UEEG	2	-19.6238	43.2475	49.8441	45.9155
Topp–Leone	1	-23.6180	49.2360	52.5343	50.5700
Unit Lindley	1	-25.1155	52.2310	55.5293	53.5650

Table 6 reports the number of fitted parameters k, the maximized log-likelihood values, and the information criteria AIC, BIC, and HQIC. All criteria were computed using the same response variable, namely anxiety (y), with a sample size of $n = 200$. Therefore, the likelihood-based criteria are directly comparable across the candidate unit distributions.

8. Fitted Regression Model

After determining the most appropriate distribution for the data, it is necessary to compare the proposed regression model with competing regression models using standard model selection criteria. The following table presents the estimated regression coefficients together with the model selection statistics.

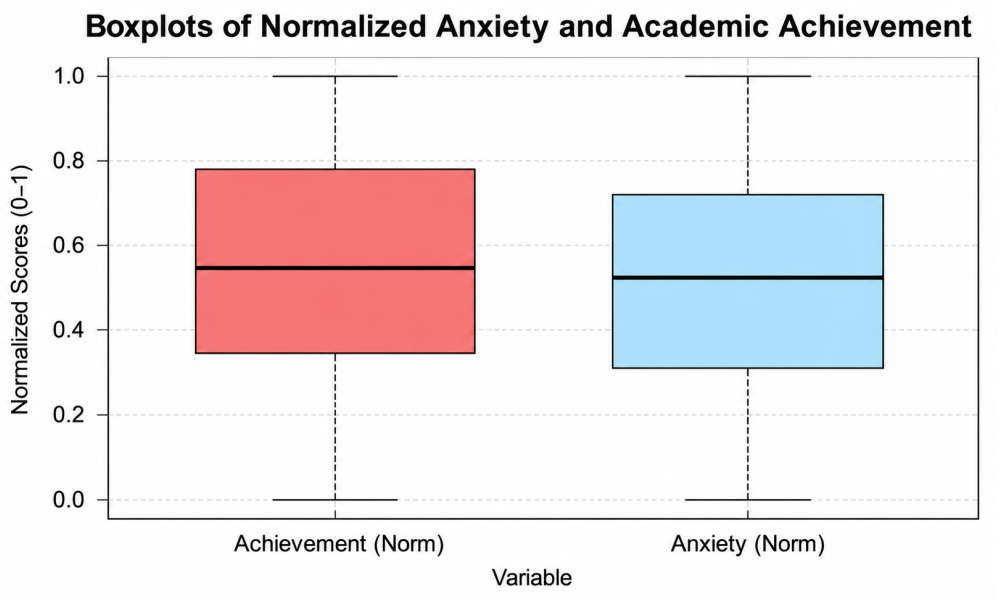

Figure 15. Boxplots of Normalized Anxiety and Academic Achievement

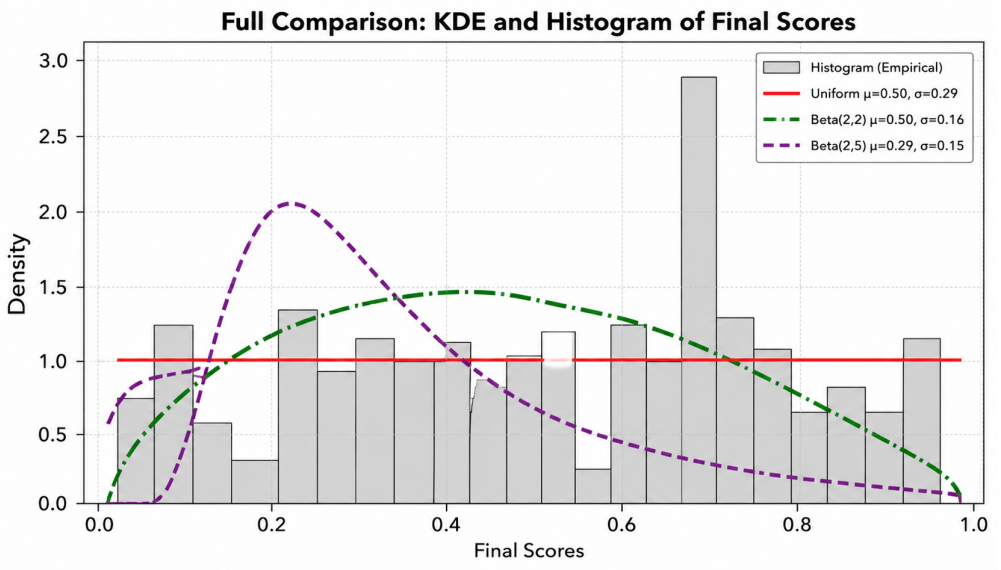

Figure 16. Full Comparison KDE and Histogram of Final Scores

Table 7. AIC, BIC, Log-Likelihood, k, and R^2 for Different Regression Models

Model	β_0	β_1	**k**	$\log$ **Lik**	**AIC**	**BIC**	$\mathbf{R^2}$
UEEG Regression	0.452	0.745	3	-48.163	102.325	112.220	0.952
Topp–Leone Regression	0.354	0.632	3	-48.618	103.236	113.131	0.785
Unit Lindley Regression	0.437	0.442	3	-49.665	105.329	115.224	0.742

Table 7 reports the regression coefficient estimates, the number of parameters k, the maximized log-likelihood values, and the corresponding information criteria AIC and BIC, together with the coefficient of determination R^2. The information criteria were computed according to

$$\mathrm{AIC} = -2\hat{\ell} + 2k$$

and

$$\mathrm{BIC} = -2\hat{\ell} + k\log(n),$$

where $n = 200$. Among the competing regression models, the proposed UEEG regression model achieved the smallest AIC and BIC values, indicating that it provides the best overall fit for the observed data. Furthermore, the UEEG regression model attained the highest R^2 value, suggesting superior explanatory power relative to the alternative regression specifications.

9. Conclusions

The current study proposed a new regression model called the Unit Extended Exponential-Geometric (UEEG) Regression Model. The maximum likelihood estimation method was employed to estimate the unknown parameters of the proposed model.

A simulation study was conducted to evaluate the finite-sample performance of the estimators, and the results demonstrated that the maximum likelihood estimation method performed efficiently, particularly in the case of small samples. Furthermore, the simulation results confirmed the consistency and stability of the estimators as the sample size increased.

The proposed regression model was also compared with competing regression specifications, namely the Unit Lindley regression model and the Topp–Leone regression model, using the Akaike Information Criterion (AIC) and Bayesian Information Criterion (BIC). According to the empirical results, the proposed UEEG regression model achieved the smallest information criteria values, demonstrating better performance and a more adequate fit than the competing models.

Overall, the findings of this study suggest that the proposed UEEG regression model provides a flexible and effective framework for modeling unit interval data and quantile-based regression structures.

Appendix A. Competing Models Used in the Model Comparison

This appendix defines the competing models used in Tables 6 and 7 so that the likelihood comparisons are reproducible. In all regression models, the conditional quantile parameter μ_i lies in the interval $(0, 1)$ and is linked to the explanatory covariates through the logit link function

$$\mathrm{logit}(\mu_i) = \mathbf{x}_i^T \boldsymbol{\beta},$$

or equivalently,

$$\mu_i = \frac{\exp(\mathbf{x}_i^T \boldsymbol{\beta})}{1 + \exp(\mathbf{x}_i^T \boldsymbol{\beta})}.$$

The log-likelihood function is defined as

$$\ell = \sum_{i=1}^{n} \log f(y_i; \mu_i, \eta),$$

where η denotes the additional shape parameter(s) associated with the corresponding distribution.

A.1 Unit Lindley Model

For $0 < y < 1$ and $\theta > 0$, the Unit Lindley probability density function is given by

$$f_{UL}(y;\theta) = \frac{\theta^2}{1+\theta}(1-y)^{-3}\exp\left(-\frac{\theta y}{1-y}\right).$$

Its cumulative distribution function is

$$F_{UL}(y;\theta) = 1 - \left[1 + \frac{\theta y}{(1+\theta)(1-y)}\right]\exp\left(-\frac{\theta y}{1-y}\right).$$

The quantile function $Q_{UL}(\tau;\theta)$ is obtained by solving

$$F_{UL}(Q;\theta) = \tau,$$

which is evaluated numerically in practical computation. In the regression setting, the parameter θ_i is replaced through a quantile-based parameterization satisfying

$$Q_{UL}(\tau;\theta_i) = \mu_i,$$

together with the regression structure

$$\text{logit}(\mu_i) = \mathbf{x}_i^T\boldsymbol{\beta}.$$

A.2 Topp–Leone Model

For $0 < y < 1$ and $\alpha > 0$, the Topp–Leone density function is defined as

$$f_{TL}(y;\alpha) = 2\alpha(1-y)\left[y(2-y)\right]^{\alpha-1},$$

with cumulative distribution function

$$F_{TL}(y;\alpha) = \left[y(2-y)\right]^{\alpha}.$$

Its quantile function is given by

$$Q_{TL}(\tau;\alpha) = 1 - \sqrt{1-\tau^{1/\alpha}}.$$

In the regression formulation, the parameter α_i is reparameterized so that

$$Q_{TL}(\tau;\alpha_i) = \mu_i,$$

while the conditional quantile parameter satisfies

$$\text{logit}(\mu_i) = \mathbf{x}_i^T\boldsymbol{\beta}.$$

REFERENCES

1. Abdullah, M. M. and Masmoudi, A. (2023). Modeling real-life data sets with a novel G family of continuous probabilistic distributions: statistical characteristics and copulas. *Pakistan Journal of Statistics and Operation Research*, 19(4), 719–746.
2. Abdulah, M., Farhan, A., Alrawi, Z., Abbood, M., & Salih, A. (2026). A Novel Compound G-Family: Statistical Characteristics and Applications to Aircraft Windshield Service Durations and Survival Time Data. *Statistics, Optimization & Information Computing*, 15(6), 4682–4698.
3. Abdulhadi, D., Ibrahim, W., Al-Saffar, R., Abd, H., & Salih, A. (2025). Performance of the Generalized shrinkage Estimator in Zero-Inflated Bell Regression Model. *Statistics, Optimization & Information Computing*, 15(4), 2488–2497.

4. Al-Doori, A. M., Salih, A., Mohammed, S. M. and Abdelfattah, A. M. (2025). Regression model for MG gamma Lindley with application. *Journal of Applied Probability & Statistics*, 20(2).
5. Altun, E., Alizadeh, M., Cordeiro, G. M., & Ozel, G. (2020). A new improved second-degree Lindley distribution with applications. *Journal of Statistical Computation and Simulation*, 90(3), 515–534.
6. Altun, E., Korkmaz, M. Ç., & Cordeiro, G. M. (2021). Regression modeling with flexible Weibull-type distributions. *Communications in Statistics – Theory and Methods*, 50(15), 3505–3524.
7. Altun, E., Ozel, G., & Alizadeh, M. (2023). The Zografos–Balakrishnan Burr XII regression model with applications. *Journal of Applied Statistics*, 50(6), 1289–1307.
8. Arslan, O., & Yu, K. (2025). Unit-Cauchy quantile regression for proportions and fractional data. *Hacettepe Journal of Mathematics and Statistics*, 54(1), 1–18.
9. Bashir, S., Ahmad, M., & Khan, M. S. (2024). A bounded exponentiated Weibull distribution with applications to unit data. *Scientific Reports*, 14, Article 65057.
10. Benkhelifa, L. (2022). The log-beta power Muth distribution with regression modeling. *Communications in Statistics – Simulation and Computation*, 51(10), 5661–5678.
11. Chanasriphum, J., Bodhisuwan, W., & Volodin, A. (2019). The log-beta generalized Weibull regression model for lifetime data. *Journal of Statistical Theory and Practice*, 13(3), 1–18.
12. Cordeiro, G. M., Ortega, E. M. M., & da Cunha, D. C. (2012). The exponentiated generalized class of distributions. *Journal of Data Science*, 10(1), 1–27.
13. Cordeiro, G. M., Ortega, E. M. M., & Silva, G. O. (2015). The log-generalized modified Weibull regression model. *Communications in Statistics – Theory and Methods*, 44(6), 1292–1310.
14. Gallardo, D. I., & Gómez, Y. M. (2021). Parametric quantile regression models for double-bounded data. *Statistics and Its Interface*, 14(4), 567–583.
15. Gómez, Y. M., & Gallardo, D. I. (2025). Exponentiated Weibull quantile regression with cure rate and applications. *Statistical Methods in Medical Research*. Advance online publication.
16. Granzotto, D. C. T., Louzada, F., & Balakrishnan, N. (2018). Transmuted Weibull regression model: Inference and applications. *Journal of Statistical Computation and Simulation*, 88(7), 1301–1318.
17. Hussein, J., Salih, A. and Abdullah, M. (2025). A deep neural network approach for estimating time-varying parameters in ordinary differential equation models. *Journal of Applied Probability & Statistics*, 20(2).
18. Jodrá, P., & Jiménez-Gamero, M. D. (2020). Quantile regression based on the exponential–geometric distribution. *REVSTAT – Statistical Journal*, 18(3), 369–389.
19. Júnior, A. F. S., Bourguignon, M., & Cordeiro, G. M. (2021). Log-generalized inverse Weibull regression model with applications. *Journal of Applied Statistics*, 48(9), 1674–1693.
20. Khan, M. S. (2021). Exponentiated Weibull regression model with applications. *Journal of Applied Statistics*, 48(4), 721–737.
21. Korkmaz, M. Ç. (2021). Exponential-power quantile regression for bounded data. *Mathematics*, 9(21), 2634.
22. Korkmaz, M. Ç., Chesneau, C., & Yousof, H. M. (2023). Unit-Chen quantile regression model with applications. *AIMS Mathematics*, 8(1), 1240–1263.
23. Maruotti, A., Rydén, T., & Tzavidis, N. (2020). Finite mixture quantile regression for semi-continuous linguodental data. *Statistical Methods in Medical Research*, 29(11), 3313–3329.
24. Mazucheli, J., Menezes, A. F. B., & Chakraborty, S. (2021). Quantile regression for bounded data based on the Birnbaum–Saunders distribution. *Statistical Papers*, 62(4), 1861–1884.
25. Mazucheli, J., Santana, T. V. F., & Menezes, A. F. B. (2022). Parametric quantile regression models: A review with applications. *Computational Statistics & Data Analysis*, 173, 107497.
26. Mazucheli, J., Santana, T. V. F., & Alves, D. C. (2023). Unit generalized half-normal quantile regression with applications. *Statistics and Computing*, 33, 34.
27. Nadarajah, S., & Kotz, S. (2006). The beta exponential distribution. *Reliability Engineering & System Safety*, 91(6), 689–697.
28. Salih, A. and Hussein, W. J. (2025). Quasi Lindley regression model residual analysis for biomedical data. *Statistics, Optimization & Information Computing*, 14(2), 956–969.
29. Salih, A., Husien, W. and Abdulah, M. (2025). High order statistics from Lambert–Topp–Leone distribution: statistical properties and applications. *Statistics, Optimization & Information Computing*, 14(3), 1584–1597.
30. Santoro, K. R., Mazucheli, J., & Menezes, A. F. B. (2024). Unit-power half-normal quantile regression with applications in health data. *Mathematics*, 12(9), 599.
31. Sánchez, L. J., Gallardo, D. I., & Gómez, Y. M. (2021). Weibull-based quantile regression with diagnostic analysis. *Mathematics*, 9(21), 2768.
32. Saulo, H., Leão, J., & Bourguignon, M. (2020). Log-symmetric quantile regression models. *Journal of Statistical Planning and Inference*, 206, 82–98.
33. Wu, S., & Rui, Y. (2025). Quantile residual life regression under length-biased censoring. *Scientific Reports*, 15, Article 93790.